Emergence of Minimal Circuits for Indirect Object Identification in Attention-Only Transformers

Rabin Adhikari
Saarland University
66123 Saarbrücken
raad00002@stud.uni-saarland.de

Abstract

Mechanistic interpretability aims to reverse-engineer large language models (LLMs) into human-understandable computational circuits. However, the complexity of pretrained models often obscures the minimal mechanisms required for specific reasoning tasks. In this work, we train small, attention-only transformers from scratch on a symbolic version of the Indirect Object Identification (IOI) task—a benchmark for studying coreference—like reasoning in transformers. Surprisingly, a single-layer model with only two attention heads achieves perfect IOI accuracy, despite lacking MLPs and normalization layers. Through residual stream decomposition, spectral analysis, and embedding interventions, we find that the two heads specialize into additive and contrastive subcircuits that jointly implement IOI resolution. Furthermore, we show that a two-layer, one-head model achieves similar performance by composing information across layers through query-value interactions. These results demonstrate that task-specific training induces highly interpretable, minimal circuits, offering a controlled testbed for probing the computational foundations of transformer reasoning.

1 Introduction

Large Language Models (LLMs) have achieved remarkable success across a vast range of natural language processing tasks [3, 12, 17]. Yet, their internal operations remain largely opaque, motivating the field of mechanistic interpretability, which seeks to reverse-engineer these "black boxes" into understandable circuits and algorithms [4, 9, 11]. The ultimate goal is to achieve a circuit-level understanding where individual components like neurons and attention heads are mapped to specific algorithmic roles [4, 5]. However, the immense scale, residual connections, and non-linearities of modern LLMs present significant challenges to this endeavor.

To navigate this complexity, researchers often start with simplified or "toy" models as controlled environments for developing and validating interpretability tools [6, 9, 19]. By training models on constrained, synthetic objectives, we can reduce confounding variables from complex linguistic structures and discover core computational mechanisms in a cleaner setting.

A common approach to understanding these models involves analyzing pre-trained transformers [18] on specific tasks they can perform [1, 2]. Wang et al. [19] introduced the Indirect Object Identification (IOI) task as a benchmark for studying such capabilities. In a typical IOI sentence, an initial dependent clause introduces two names (a subject, S, and an indirect object, IO), and the main clause repeats the subject. The task is to predict the IO as the final token. Wang et al. [19] showed that GPT-2 small [13] implements IOI through a multi-hop attention circuit involving distinct classes of heads. However, this mechanism arises within a model pretrained for next-token prediction on natural text—an inherently complex optimization setting.

In contrast, we train minimal, attention-only transformer models [18] from scratch exclusively on a symbolic version of the IOI task. We find that a straightforward model—a single-layer transformer with just two attention heads—can solve this task perfectly. Since we know that the task of IOI can't be performed using a skip-gram model, our argument is similar in spirit to Shlegeris [14] that a one-layer attention-only transformer has a higher representational capacity than a skip-gram. Furthermore, a detailed analysis of this model uncovers a highly compact and interpretable circuit where the solution is computed via a direct additive combination of the two heads' outputs, rather than a complex, multi-hop pipeline.

Our contributions are threefold:

1. We demonstrate that a one-layer, two-head attention-only model is sufficient to solve the IOI task with a fixed template perfectly.

2. We provide a mechanistic analysis that uncovers a minimal circuit based on an additive combination of specialized attention head outputs.

3. We argue that the circuits in large, broadly pre-trained models may be overly complex due to multi-task pressures, whereas task-constrained training can reveal more parsimonious mechanisms.

2 Dataset and Model Configuration

2.1 The IOI Task in a Symbolic Setting

To isolate the core relational reasoning challenge of the IOI task, we construct a symbolic dataset that abstracts away all linguistic and tokenization complexities. The task remains to identify the correct indirect object (IO) from the dependent clause, given a subject (S) from the main clause, but now these are simply names drawn from a small vocabulary. This formulation abstracts the essential relational pattern from the natural-language IOI task—"When John and Mary ... John gave ... to ___"—while removing all linguistic confounds. It enables precise inspection of what the model must represent to distinguish between "subject" and "object" roles.

The training data consists of 6-token sequences built from two primary templates. Using "John" (S) and "Mary" (IO) as examples:

1. `<BOS> John Mary Mary <MID> John`

2. `<BOS> John Mary John <MID> Mary`

Here, `<BOS>` marks the start of the sequence, and the model's objective is to predict the IO token at the final position, following the `<MID>` token. The two names are drawn randomly from a vocabulary of six names, and the correct final token is chosen uniformly at random.

2.2 Model Configuration

To maximize interpretability, we used simple attention-only transformer models. Feed-forward networks and layer normalization were omitted to isolate the function of the attention mechanism. The vocabulary consists of 6 name tokens plus the two special tokens `<BOS>` and `<MID>`, for a total size of 8. The residual stream dimension was set to 8, and the head dimension was $d_{head} = \frac{8}{N_h}$, where N_h is the number of heads.

Training: Models were trained from scratch on the symbolic IOI dataset using a cross-entropy loss to predict the token at the `<MID>` position. Each training batch contained all 60 possible unique sequences ($6 \times 5 \times 2 = 60$). We used the AdamW optimizer [7] with a OneCycle learning rate scheduler [15], a maximum learning rate of 0.1, and weight decay of 0.01. Training and analyses were performed on a single NVIDIA A40 GPU using the *TransformerLens* [8] library.

3 Results and Analysis

3.1 Single-Head, One-Layer Model Fails to Learn

A single attention head outputs $\approx 50\%$ probability for the names provided in the prompt, indicating that the model knows that the final answer is one of the two names provided. But it cannot distinguish which one is correct. The model attends roughly equally to both the names in the dependent clause (see figure 1a), indicating that a single attention head cannot jointly encode the information required to **(i)** identify which token serves as the correct referent and **(ii)** propagate that information to the prediction position. The roles of "reference detection" and "copying" appear to be functionally incompatible within a single attention mechanism.

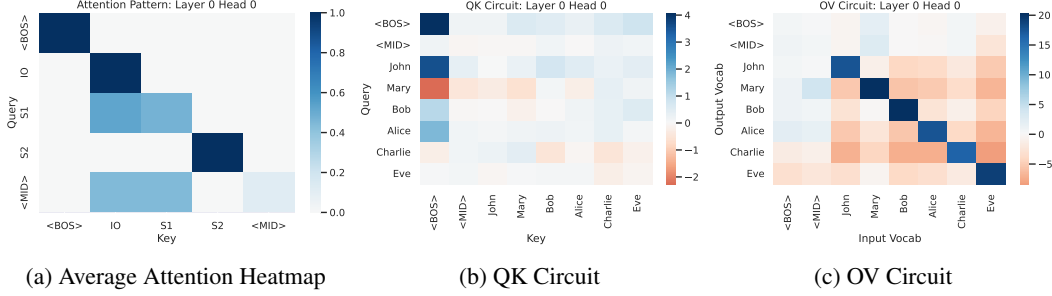(a) Average Attention Heatmap (b) QK Circuit (c) OV Circuit

Figure 1: **Single-Head, One-Layer Model Fails to Learn IOI.** (a) The attention heatmap showing the <MID> token attends uniformly to the two names. (b) The QK circuit reveals that the <MID> token attends uniformly to all tokens. (c) The OV circuit shows that each name token has a large positive contribution to its own logit and a small negative contribution to the other name's logit.

Following Elhage et al. [5], we analyze the QK and OV circuit to understand the failure mode of the single-head model. From the QK circuit (see figure 1b), we observe that the <MID> token attends almost uniformly to all tokens. And from the OV circuit (see figure 1c) shows that each name token makes a high positive contribution to its own logit but a small negative contribution to the logit of the other name. Due to the uniform attention pattern, these contributions average out, resulting in similar logits for both names.

3.2 Two-Head, One-Layer Model Learns IOI Perfectly

When the model is extended to two attention heads, it achieves perfect accuracy on the IOI task. Figure 2 shows distinct attention patterns of the two heads, averaged across all the possible inputs.
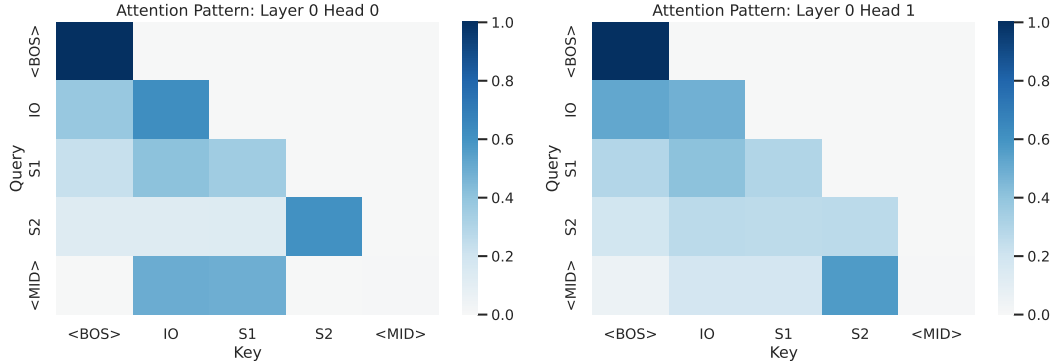

Figure 2: **Average Attention Heatmap for Two-Head, One-Layer Model.** Head 0 focuses almost equally on the two name tokens from the dependent clause, while Head 1 has half of its attention on the subject of the main clause and almost a quarter on each of the names in the dependent clause.

3

3.2.1 Two Heads with Distinct Roles

We observed that, for both the templates of our symbolic dataset, the first head consistently attends to the two names in the initial dependent clause (see figure 2), indicating its role in identifying the relevant referents. The second head, however, always attends to the subject of the main clause and the other name in the dependent clause — "BA" in the "BAAB" template and similarly, "AB" in the "BABA" template (see figure 3). So, this head does the most of the heavy lifting, finding out the unique set of tokens to attend to. Furthermore, it suggests that the second head is responsible for integrating the referential information with the context provided by the main clause to determine the correct output.
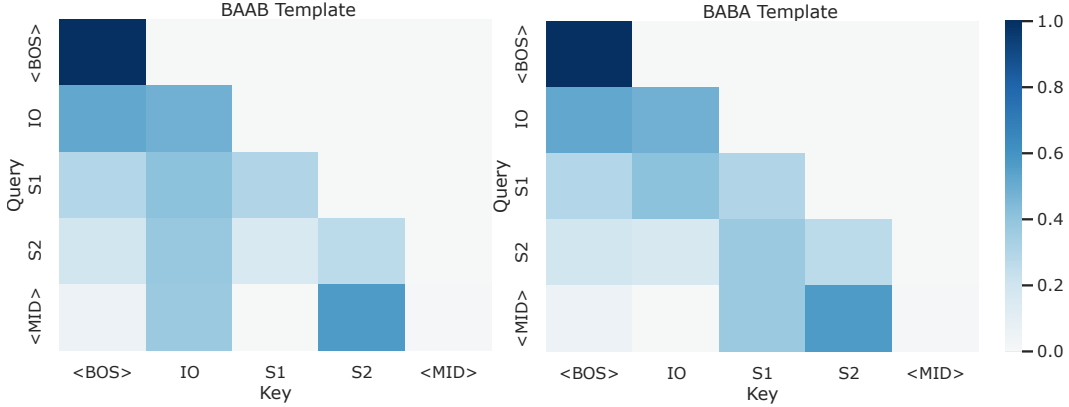

Figure 3: **The attention map for the second head depends on the template.** While the first head always attends to the two name tokens in the dependent clause, the second head attends to the second occurrence of the subject in the main clause and the other name in the dependent clause — "BA" in the "BAAB" template and similarly, "AB" in the "BABA" template.

3.2.2 Residual Stream Decomposition

To understand how the model's components contribute to the final prediction, we decompose the residual stream at the final token position (corresponding to <MID> token) into the contributions of those components. We then project these components onto directions in the embedding space corresponding to the correct and incorrect names, as well as their sum and difference [10]. Figure 4 shows that the first head's output is aligned closest with the sum direction—that is, it represents the combined contribution of both the correct and incorrect names (*correct + incorrect*). On the other hand, the second head's output aligns closest with the direction of the token difference—the contrast between the two name embeddings (*correct – incorrect*). Since the final logits are computed by adding the contribution of all the components, the logit component for the incorrect token cancels out, and the direction corresponding to the correct token is amplified.

This analysis is also not foolproof because we can see that the second head also has some component in the direction of the correct token, as well as the sum direction. Nevertheless, we observe a clear division of labor between the two heads: one aggregates signals (additive), while the other suppresses the incorrect alternative (contrastive). Together, they form an additive-contrastive circuit to produce a clean, interpretable mechanism for generating the correct logits.

3.2.3 Spectral Analysis of QK and OV Circuits

We expect an equal number of positive and negative eigenvalues for a random matrix [16]. However, we observe a significant asymmetry in the eigenvalue distributions of both the QK and OV matrices for our two-head model. This asymmetry reinforces our hypothesis that the learned attention mechanisms have developed specialized functions. We present the eigenvalue decomposition of the QK and OV matrices in figures 5 and 6, respectively. Furthermore, on the top-right of each subfigures, we report the fraction of positive eigenvalues for each head calculated using the formula $\frac{\sum_i \lambda_i}{\sum_i |\lambda_i|}$, where λ_i are the eigenvalues of the matrix and $|\lambda_i|$ are their magnitudes.
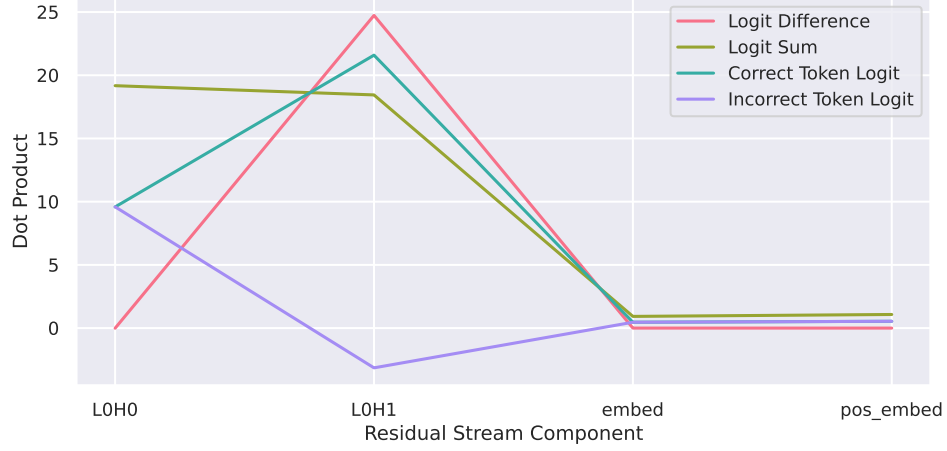
Figure 4: **Residual Stream Decomposition for Two-Head, One-Layer Model.** The dot product of the output of each of the components of the residual stream. The first head's output aligns most with the sum direction, while the second head's output aligns most with the difference direction.

Spectral Properties of QK Circuits Observing the eigendecomposition of the QK matrices (see figure 5), we note the following:

- Head 0 has a moderate suppression mechanism (≈ -5.2) to forbid attending to some dimensions (or some tokens), indicating a less pronounced inhibitory effect. And the positive fraction around zero (-0.06) suggests that the amplifying effect of the rotational component is almost balanced by the suppressive effect of the negative eigenvalue. Hence, the overall attention dynamics of Head 0 are relatively neutral.

- Head 1 has a strong suppression mechanism (≈ -17.5), indicating a more pronounced inhibitory effect. The positive fraction of -0.65 suggests that the suppressive effect of the dominant negative eigenvalue outweighs the amplifying effect of the rotational components, leading to an overall inhibitory attention dynamic.
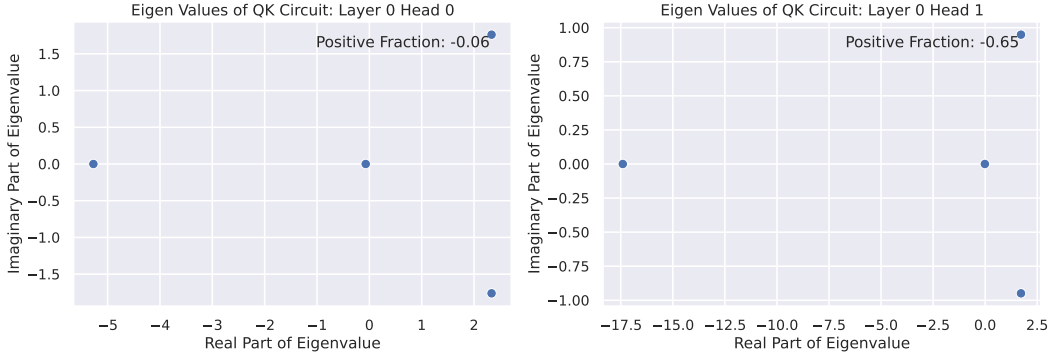

Figure 5: **Eigenvalue Distribution of QK Circuits for Two-Head, One-Layer Model.** Head 1 has a larger dominant negative eigenvalue (positive fraction of -0.65) compared to Head 0 (positive fraction of -0.06), indicating a stronger suppressive effect in Head 1's attention dynamics.

Spectral Properties of OV Circuits Eigendecomposition of the OV matrices (see figure 6) further reveals the asymmetry between the two heads:

- Head 0 is a **copying** or **passthrough** head, which identifies important tokens via its QK circuit and then amplifies their presence in the residual stream without any rotation or inversion.

5

- Head 1 has half of its eigenvalues as positive and the other half as imaginary with negative real parts. This suggests that the chosen token will copy itself in some dimension and rotate with inversion in another dimension, which can be interpreted as subtracting from the logits of the other token with some added transformations.

This distinction corresponds naturally with the roles inferred from embedding projections: one head aggregates signals (additive), while the other suppresses the incorrect alternative (contrastive).
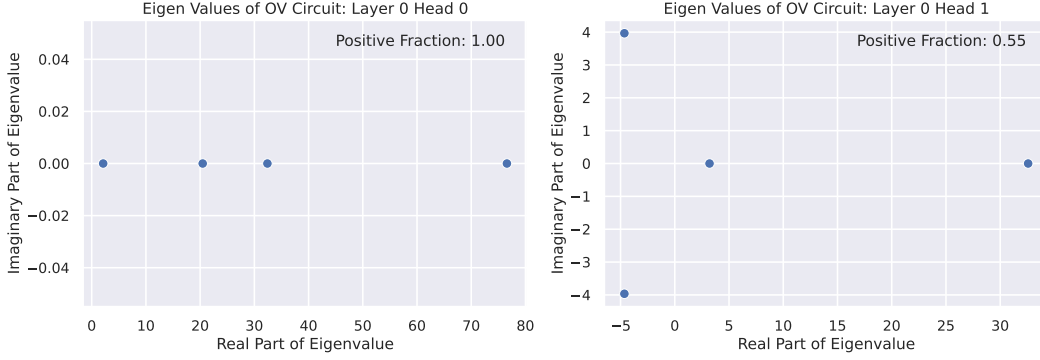

Figure 6: **Eigenvalue Distribution of OV Circuits for Two-Head, One-Layer Model.** The first head has all positive eigenvalues (positive fraction of 1), indicating an additive contribution to the residual stream. In contrast, the second head has positive as well as imaginary eigenvalues with negative real parts (positive fraction of 0.55), suggesting a mix of additive and contrastive contributions.

3.2.4 Positional Focus of Attention Heads

We take the average of all the embeddings of all the names and assign that as their common embedding to remove any semantic information from the name tokens, providing the model with only positional embeddings for the name tokens. From figure 7, we observe the following attention patterns:

- We can consider the first head as the **positional head** that focuses on the positions of the names in the dependent clause, almost independent of their word embeddings.
- The second head attends predominantly to the position of occurrence of the subject in the main clause. However, despite this positional focus, it attends to the name in the dependent cause that is other than the subject of the main clause. This indicates that the second head is responsible for integrating positional as well as contextual information to determine the correct output.
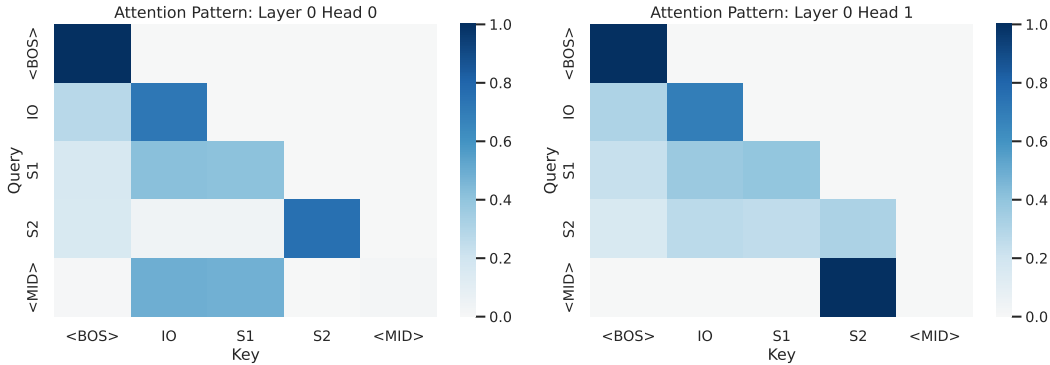

Figure 7: **Average Attention Heatmap for Two-Head, One-Layer Model with Averaged Name Embeddings.** Head 0 focuses almost equally on the positional embeddings of the two name tokens from the dependent clause, while Head 1 attends primarily to the positional embedding of the subject token of the main clause.

6

3.2.5 Ablating Positional Embeddings

To study how the model utilizes positional information, we train the same model architecture without any positional embeddings. The model achieves an accuracy of $\approx 70\%$ on the IOI task, putting $\approx 67\%$ probability on the correct token, indicating that positional embeddings are not strictly necessary for the model to learn the task, but they do enhance performance. Although both the heads trained in this manner exhibit similar attention patterns, they somehow manage to focus on the correct output name present in the dependent clause (see figure 8). So, despite the absence of explicit positional cues, the model still manages to learn a strategy that allows it to perform the task with reasonable accuracy, likely by relying more heavily on the semantic content of the name embeddings and their contextual relationships. However, adding positional embedding improves the model's accuracy to 100% and makes the internals more interpretable.
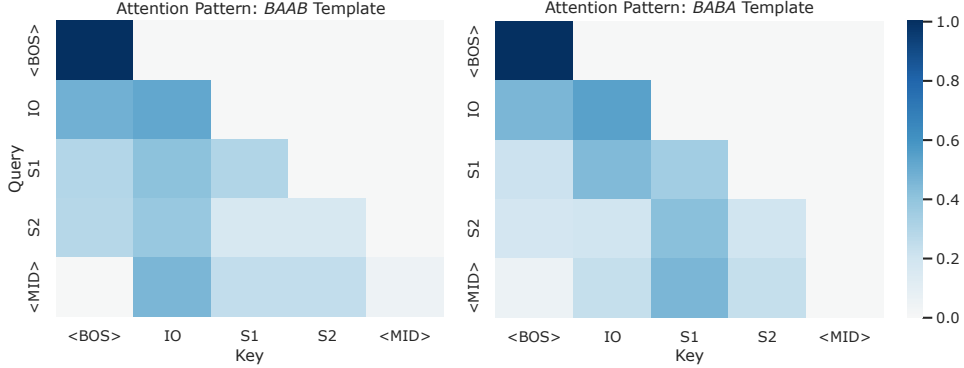

Figure 8: **Average Attention Heatmap for Two-Head, One-Layer Model trained without Positional Embeddings.** Both heads focus mostly on the correct output name present in the dependent clause, i.e., *B* in the "BAAB" template and *A* in the "BABA" template.

3.3 Two-Layer, One-Head Model and Composition

Motivation We also train a one-head, two-layer attention-only transformer to observe how a model performs IOI in the availability of compositions [5] using the output of the previous layer. The head dimension was 4 for the one-layer two-heads model, and for this model, since we have a single head per layer, the hidden dimension is the same as the hidden dimension of the one-head one-layer model, i.e., 8. So, this model has more representational capacity than the one-head one-layer model. If this model doesn't perform any composition, then it is the same as the one-layer two-heads model with each layer writing to the residual stream in orthogonal subspaces of 4 dimensions each.

Attention Pattern From figure 9, we observe that the attention patterns of both layers change depending on the template. The <MID> token in the first layer still attends to both the name tokens in the dependent clause, similar to the first head of the one-layer two-heads model. However, the S2 token in the first layer changes its attention pattern based on the template. So, the first head is not solely positional, but aggregates information to S2 token to be used by the latter head. Although the attention pattern of the second layer for the <MID> token seems almost similar to the attention pattern of the second head of the one-layer two-heads model, this time it attends to the aggregated information from the first layer.

Role of Positional Embeddings Figure 10 shows that both the heads focus on the positional embeddings of the tokens. The first head's attention pattern on the positional embeddings is similar to the pattern with the positional embeddings, indicating that it is mostly a positional head. However, although the <MID> token in the second layer attends primarily to the token before it, it changes its attention pattern based on the context provided by the first layer. So, the second head is not solely positional, but integrates positional as well as contextual information to determine the correct output.

Composition Ablation To study the type of composition that the model is performing (Q, K, or V), we ablate them one by one by subtracting the output of the first layer from the corresponding input
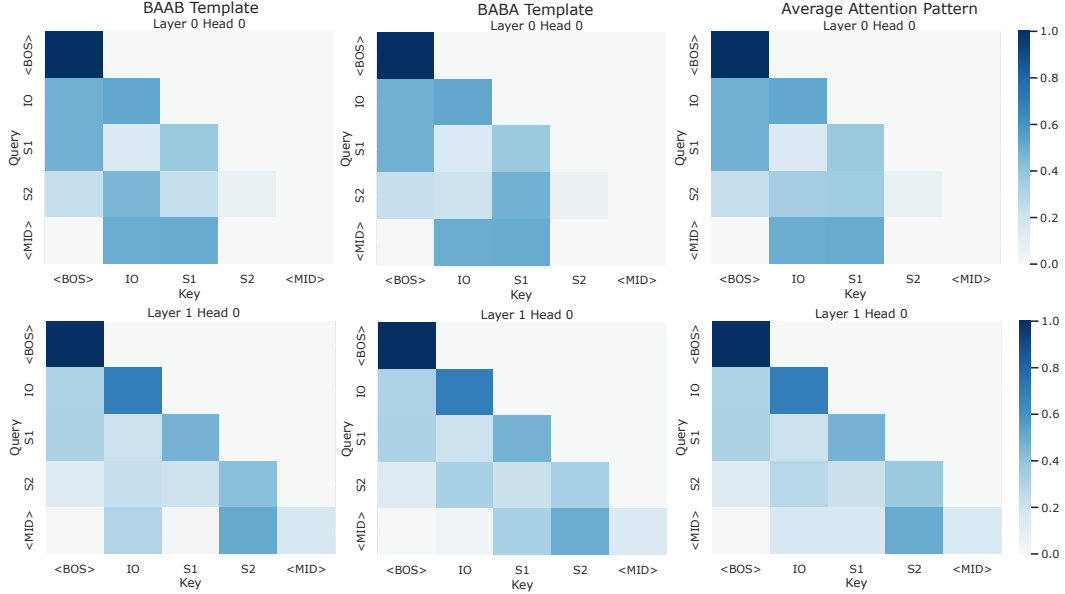
Figure 9: **Attention Heatmap for Two-Layer, One-Head Model.** The heatmap of both heads changes depending on the template.
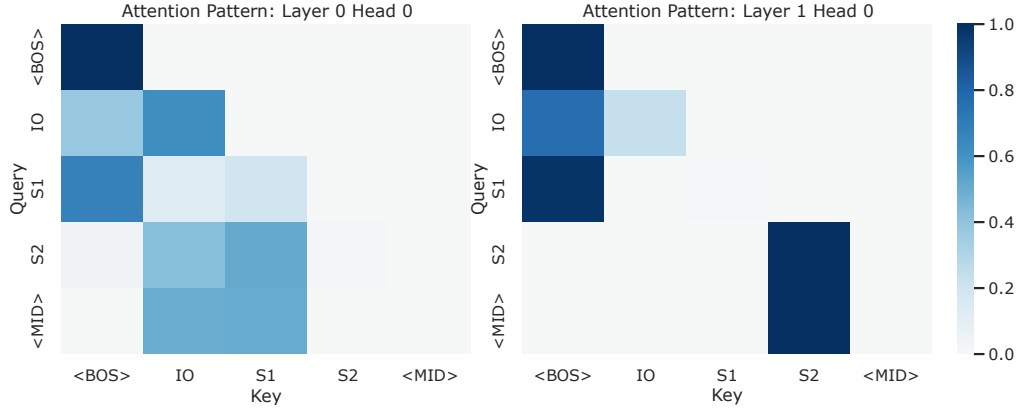

Figure 10: **Attention Heatmap for Two-Layer, One-Head Model with Averaged Name Embeddings.** We see a strong positional focus in both heads.

of the Q, K, and V matrices. We observe a drop in accuracy in the following order: Q composition ($\approx 100\%$ drop), V composition ($\approx 93.33\%$ drop), and K composition ($\approx 26.67\%$ drop). This indicates that the model is heavily relying on the Q and V compositions to perform the task. So, we can conclude that the two-layer one-head model is indeed performing some composition to solve the IOI task, different from the one-layer two-heads model.

4   Conclusion

In this study, we showed that even a minimal attention-only transformer—comprising just two attention heads—can perfectly solve a symbolic version of the Indirect Object Identification task. Our mechanistic analysis revealed an elegant division of labor: one head aggregates referential information additively, while the other performs contrastive suppression of incorrect alternatives. In a two-layer, single-head model, we further observed compositional behavior across layers, indicating the emergence of functional hierarchy. These findings highlight that task-constrained training can produce parsimonious and interpretable circuits, offering valuable insight into the primitive computational motifs that may underlie reasoning in larger, pretrained language models.

References

[1] Leonard Bereska and Stratis Gavves. "Mechanistic Interpretability for AI Safety - A Review". In: *Trans. Mach. Learn. Res.* 2024 (2024) (see page: 1).

[2] Jannik Brinkmann, Abhay Sheshadri, Victor Levoso, Paul Swoboda, and Christian Bartelt. "A Mechanistic Analysis of a Transformer Trained on a Symbolic Multi-Step Reasoning Task". In: *ACL (Findings)*. Association for Computational Linguistics, 2024, pp. 4082–4102 (see page: 1).

[3] Tom B. Brown, Benjamin Mann, Nick Ryder, Melanie Subbiah, Jared Kaplan, Prafulla Dhariwal, Arvind Neelakantan, Pranav Shyam, Girish Sastry, Amanda Askell, Sandhini Agarwal, Ariel Herbert-Voss, Gretchen Krueger, Tom Henighan, Rewon Child, Aditya Ramesh, Daniel M. Ziegler, Jeffrey Wu, Clemens Winter, Christopher Hesse, Mark Chen, Eric Sigler, Mateusz Litwin, Scott Gray, Benjamin Chess, Jack Clark, Christopher Berner, Sam McCandlish, Alec Radford, Ilya Sutskever, and Dario Amodei. "Language Models are Few-Shot Learners". In: *NeurIPS*. 2020 (see page: 1).

[4] Arthur Conmy, Augustine N. Mavor-Parker, Aengus Lynch, Stefan Heimersheim, and Adrià Garriga-Alonso. "Towards Automated Circuit Discovery for Mechanistic Interpretability". In: *NeurIPS*. 2023 (see page: 1).

[5] Nelson Elhage, Neel Nanda, Catherine Olsson, Tom Henighan, Nicholas Joseph, Ben Mann, Amanda Askell, Yuntao Bai, Anna Chen, Tom Conerly, Nova DasSarma, Dawn Drain, Deep Ganguli, Zac Hatfield-Dodds, Danny Hernandez, Andy Jones, Jackson Kernion, Liane Lovitt, Kamal Ndousse, Dario Amodei, Tom Brown, Jack Clark, Jared Kaplan, Sam McCandlish, and Chris Olah. "A Mathematical Framework for Transformer Circuits". In: *Transformer Circuits Thread* 1.1 (2021), p. 12 (see pages: 1, 3, 7).

[6] Mor Geva, Roei Schuster, Jonathan Berant, and Omer Levy. "Transformer Feed-Forward Layers Are Key-Value Memories". In: *EMNLP (1)*. Association for Computational Linguistics, 2021, pp. 5484–5495 (see page: 1).

[7] Ilya Loshchilov and Frank Hutter. "Decoupled Weight Decay Regularization". In: *ICLR (Poster)*. OpenReview.net, 2019 (see page: 2).

[8] Neel Nanda and Joseph Bloom. *TransformerLens*. Version v2.16.1. Aug. 26, 2022. URL: https://github.com/TransformerLensOrg/TransformerLens (see page: 2).

[9] Neel Nanda, Lawrence Chan, Tom Lieberum, Jess Smith, and Jacob Steinhardt. "Progress Measures for Grokking via Mechanistic Interpretability". In: *ICLR*. OpenReview.net, 2023 (see page: 1).

[10] nostalgebraist. *interpreting GPT: the logit lens*. LessWrong. Aug. 31, 2020. URL: https://www.lesswrong.com/posts/AcKRB8wDpdaN6v6ru/interpreting-gpt-the-logit-lens (see page: 4).

[11] Chris Olah, Nick Cammarata, Ludwig Schubert, Gabriel Goh, Michael Petrov, and Shan Carter. "Zoom In: An Introduction to Circuits". In: *Distill* 5.3 (2020), e00024–001 (see page: 1).

[12] OpenAI. "GPT-4 Technical Report". In: *CoRR* abs/2303.08774 (2023) (see page: 1).

[13] Alec Radford, Jeffrey Wu, Rewon Child, David Luan, Dario Amodei, and Ilya Sutskever. "Language Models are Unsupervised Multitask Learners". In: *OpenAI blog* 1.8 (2019), p. 9 (see page: 1).

[14] Buck Shlegeris. *One-layer transformers aren't equivalent to a set of skip-trigrams*. AI Alignment Forum. Feb. 18, 2023. URL: https://www.alignmentforum.org/posts/b5HNYh9ne5vEkX5ag/one-layer-transformers-aren-t-equivalent-to-a-set-of-skip (see page: 2).

[15] Leslie N. Smith and Nicholay Topin. "Super-Convergence: Very Fast Training of Residual Networks Using Large Learning Rates". In: *CoRR* abs/1708.07120 (2017) (see page: 2).

[16] Wojciech Tarnowski. "Real Spectra of Large Real Asymmetric Random Matrices". In: *Physical Review E* 105.1 (Jan. 2022), p. L012104 (see page: 4).

[17] Hugo Touvron, Thibaut Lavril, Gautier Izacard, Xavier Martinet, Marie-Anne Lachaux, Timothée Lacroix, Baptiste Rozière, Naman Goyal, Eric Hambro, Faisal Azhar, Aurélien Rodriguez, Armand Joulin, Edouard Grave, and Guillaume Lample. "LLaMA: Open and Efficient Foundation Language Models". In: *CoRR* abs/2302.13971 (2023) (see page: 1).

[18] Ashish Vaswani, Noam Shazeer, Niki Parmar, Jakob Uszkoreit, Llion Jones, Aidan N. Gomez, Lukasz Kaiser, and Illia Polosukhin. "Attention is All you Need". In: *NIPS*. 2017, pp. 5998–6008 (see pages: 1, 2).

[19] Kevin Ro Wang, Alexandre Variengien, Arthur Conmy, Buck Shlegeris, and Jacob Steinhardt. "Interpretability in the Wild: A Circuit for Indirect Object Identification in GPT-2 Small". In: *ICLR*. OpenReview.net, 2023 (see page: 1).